maximum, amounts to $u_0 = L/(p_0/\dot{p}_0)$. The corresponding Reynolds number, which also is maximum at the inlet station, is a function of the tube length-diameter product: $R_N = |\dot{p}_0 Ld/(\mu RT)|$, where R and T are the gas constant for air and the tube temperature, respectively. Both the Reynolds number and the fluid velocity at the tube entrance maintain proportionality to the rate of change of the applied pressure, but the Reynolds number, unlike the velocity, does not depend explicitly on the pressure level.

The tube entrance length required to produce the assumed state of fully-developed flow is dependent on Reynolds number. Boussinesq, as reported by Daily and Harleman,[3] obtained theoretically a length estimate for steady laminar flow that agrees well with experiment: $(L/d)_{\text{entrance}} = 0.065 R_N$. In the present work, the tube is taken to be long compared with this dimension.

Acknowledgment

This work was supported by the U.S. Department of Energy under Contract DE-AC04-76DP00789.

References

[1]Ducoffe, A.L., "Pressure Response in Supersonic Wind-Tunnel Pressure Instrumentation," *Journal of Applied Physics,* Vol. 24, Nov. 1953, pp. 1343-1354.

[2]Sato, J., "Settling Times of Pressure Measurements through Capillary Tubes," *AIAA Journal,* Vol. 17, Oct. 1979, pp. 1061-1067.

[3]Daily, J.W. and Harleman, D.R.F., *Fluid Dynamics,* 2nd printing, Addison-Wesley, Reading, Massachusetts, 1973, p. 260.

Drag Reduction of Perforated Axisymmetric Bodies in Supersonic Flow

Eugen Serbănescu* and George Savu*
The National Institute for Scientific and Technical Creation
Bucharest, Romania

Nomenclature

B = $\sqrt{M^2-1}$
C_{Dp} = pressure drag coefficient
C_p = pressure coefficient
$f(x)$ = porosity function
L^* = maximal axial dimension of the body
M_∞ = freestream Mach number
p, p_t = nondimensional state and total pressures, p^*/p^*_∞ and p^*_t/p^*_∞, respectively
Re = reference Reynolds number
S = $\pi r^2_{\max}$
U_∞ = freestream velocity
u, v = nondimensional axis and radial perturbance velocities, u^*/U^*_∞ and v^*/U^*_∞, respectively
v_n = nondimensional normal surface velocity, v^*_n/U^*_∞
ϵ = thickness ratio of parabolic-arc spindle, $2r^*_{\max}/L^*$
θ^* = cone half-angle
ρ = nondimensional fluid density, ρ^*/ρ^*_∞
σ = nondimensional porosity factor, $\sigma^* U^*_\infty/p^*_\infty$

Superscripts and Subscripts

( )* = dimensional parameter
( )′ = derivative
∞ = undisturbed conditions
e = equivalent solid body
max = maximal
p = plenum chamber

Received Feb. 6, 1984; revision received Jan. 7, 1985.

*Research Scientist, Aerodynamics Department.

Introduction

THE optimization of aerodynamic body profiles relating to drag reduction has become a current effort in aerodynamics. The well-known shapes of the minimum drag bodies of revolution (Sears-Haack body, von Kármán ogive, Lighthill body, etc.) reach their optimum at a single flight Mach number, the one called "on-design."

The idea we propose in the present Note leads to an aerodynamic drag reduction not only of the "on-design" point, but also "off-design" points, based on the use of perforated surfaces. As a matter of fact, a numerical treatment of a *self-adapting aerodynamical system* useful for axisymmetric bodies is presented. This implies both massive suction and massive blowing through the axisymmetric perforated surface. The theoretical framework (large rate of mass transfer through perforated surfaces) is the same as earlier research.[1-4] However, in our proposal, the existence of a cavity (plenum chamber) within the perforated surface is considered, so that a secondary (plenum) flow could be born due to the difference between the pressures acting "naturally" on the connected zones of the body (Fig. 1). No appropriate installation, device, or pump is imposed. *The system works itself.* As a consequence, a new pressure distribution will occur as the result of the interaction between the outer (main) and inner (secondary/plenum) flow. This interaction is allowed and conrolled by the distribution and inclination of the perforated surface holes as well as by the size of the holes to the cavity wall thickness ratio. (All of these parameters are incorporated into the porosity coefficient σ).

In this Note the normal velocity on the perforated surface is no more imposed, as in other works,[1-4] but is the result of the above aerodynamic mechanism and governed by the Darcy law (accepted in the mass transfer through the perforated walls case).[5]

A point of view similar to Refs. 1-4 has been adopted regarding the principal effect of the massive mass transfer which is considered inviscid because the normal velocity v_n can be much larger than the usual order of magnitude (0.0001-0.01) required for the consistency of boundary-layer theory,[6] i.e.,

$$v_n \gg Re^{-1/2}$$

The physical phenomenon is similar to that which takes place in wind tunnel test section with perforated walls, where the viscous effect is also negligible.

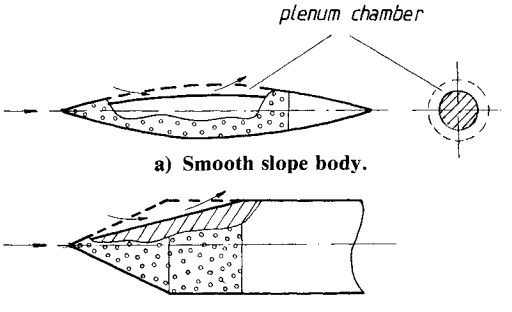

a) Smooth slope body.

b) Cone-cylinder ogive.

Fig. 1 Bodies of revolution with a perforated surface.

Analysis

Consider a supersonic flow around an axisymmetric body. Using small-disturbance theory, the potential φ of the steady inviscid motion is given by

$$(M_\infty^2 - 1)\varphi_{xx} - \varphi_{rr} - \varphi_r/r = 0 \tag{1}$$

with the boundary conditions

$$v_n^* = 0 \quad \text{for the unperforated surface} \tag{2}$$

$$v_n^* = \sigma^*(p^* - p_p^*) \quad \text{for the perforated surface (Darcy law)} \tag{3}$$

To solve Eq. (1), the von Kármán-Moore method[7] has been chosen, taking into account the possibility of this method to be applied to both smooth and rough axisymmetric bodies.[8]

The distribution of supersonic axial sources gives the following disturbance velocities at x_i:

$$u_i = \sum_{k=2}^{i} C_k \{\operatorname{argch}[(x_i - \xi_k)/B/r_i] - \operatorname{argch}[(x_i - \xi_{k-1})/B/r_i]\} \tag{4}$$

$$v_i = -\sum_{k=2}^{i} C_k \left[\sqrt{(x_i - \xi_k)^2 - B^2 r_i^2} - \sqrt{(x_i - \xi_{k-1})^2 - B^2 r_i^2}\right]/r_i \tag{5}$$

where $i = 2,3,\ldots,n-1$, n and

$$\xi_k = x_k - Br_k \tag{6}$$

The C_k constants are determined from boundary condition equations (2) and (3), which can be written in "small perturbances" as

$$v_i = (1 + u_i)r_i' \tag{7}$$

and, for

$$v_i = (1 + u_i)r_i' - \sigma(u_i - u_p) \tag{8}$$

In Eq. (8) u_p denotes a fictitious disturbance velocity corresponding to the plenum chamber pressure p_p which, in the first approximation, is assumed to be constant inside the plenum chamber (the plenum chamber does not communicate with the outward flow except through the perforated surface). Thus u_p can be found from the vanishing condition of the mass flow rate through the entire perforated surface.

$$\int_0^{2\pi}\int_0^1 \rho v_n \, dx \, d\omega = 0 \tag{9}$$

From Eqs. (8) and (9) we extract the magnitude of u_p

$$u_p = \int_0^{2\pi}\int_0^1 ur\rho\sigma \, d\omega dx \Big/ \int_0^{2\pi}\int_0^1 r\rho\sigma \, d\omega dx \tag{10}$$

where

$$\rho \cong 1 - uM^2 \tag{11}$$

The procedure is an iterative one with the values of perturbation velocities u_i from the previous iteration being used for the computation of a new value of u_p, which, introduced in the boundary condition (8), yields a new set of C_k, and implicitly a new set of u_i, up to the required accuracy.

The pressure distribution acting on the perforated body is now used to create a solid equivalent body having the contour

$$r_e(x) = \int_0^x r_e'(\eta) \, d\eta \tag{12}$$

as it results from the conditions

$$2u_e + v_e^2 = -C_p \tag{13}$$

$$v_e/(1 + u_e) = r_e' \tag{14}$$

where u_e and v_e have the form of Eqs. (4) and (5).

This equivalent solid body allows us to calculate the drag resulting from the given pressure distribution, i.e., the drag of the perforated body.

Results and Conclusions

Numerical experiments on several axisymmetric pointed bodies and at various Mach numbers have been done.

The pressure distribution on a solid and perforated parabolic body, with $\epsilon = 1/6$ and the wave drag variation vs Mach number plotted in Fig. 2. In Fig. 2b, one may notice that if the solid equivalent body of a certain Mach number (on-design point) evolves at other Mach numbers (off-design points), then its wave drag has a larger value than the equivalent solid body at those corresponding Mach numbers. It can be said that perforating the surface is similar to optimizing the drag reduction in a large range of Mach numbers.

An important application of this concept seems to be a perforated cone-cylinder body. In this case, the expansion behind the cone-cylinder joint yields the suction of the stream through the conical surface and its blowing through the cylinder surface.

In Fig. 3a, it is remarkable that the pressure jump of the solid body is reduced considerably if the zone is perforated [$f(x) = \sin^2(\pi x)$]. Hence, the corresponding equivalent body outline is a nearly smooth function, as a consequence of the fact that perforated surfaces do not allow pressure jumps.

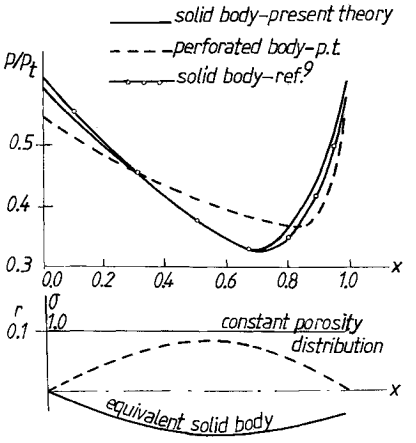

a) Pressure distribution.

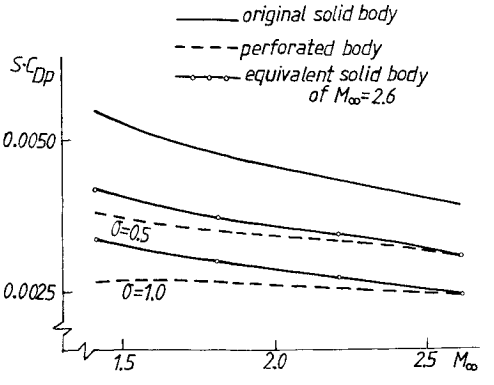

b) Drag variation vs Mach numbers.

Fig. 2 Parabolic-arc spindle with $\epsilon = 1/6$ at $M_\infty = 1.15$.

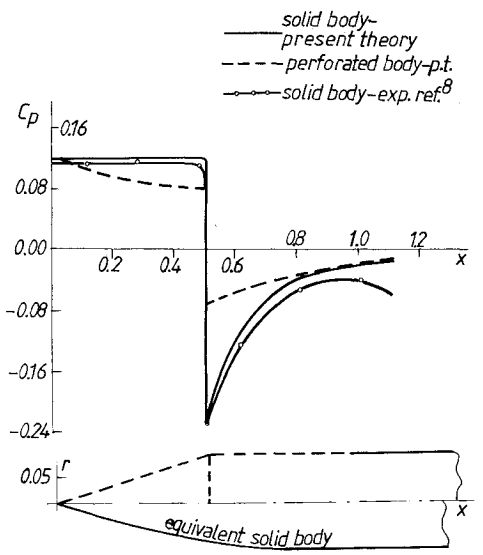

a) Pressure coefficient distribution.

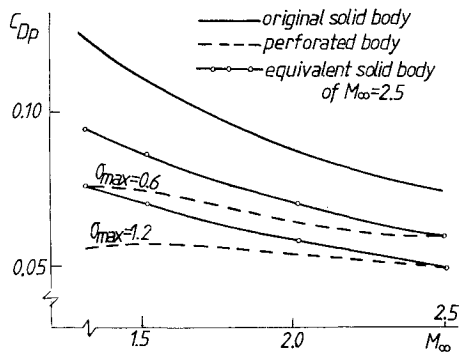

b) Drag variation vs Mach numbers.

Fig. 3 Cone-cylinder ogive with $\theta^* = 10$ deg at $M_\infty = 1.32$.

This study can be improved by assuming a more complex physical model and/or by using a more accurate theory. On the other hand, experimental data are expected to be in good agreement with the results presented herein.

References

[1]Aroesty, J. and Davis, S.H., "Inviscid Cone Flows with Surface Mass Transfer," *AIAA Journal,* Vol. 4, Oct. 1966, pp. 1830-1832.

[2]Emanuel, G., "Blowing from a Porous Cone or Wedge When the Contact Surface is Straight," *AIAA Journal,* Vol. 5, March 1967, pp. 534-538.

[3]Ismail, A. and Ting, L., "Large Rate of Injection Normal to Surface in High Speed Flow," *Astronautica Acta,* Vol. 14, 1969, pp. 653-663.

[4]Carafoli, E., Berbente, C., and Serbănescu, E., "On the Total Axial-Symmetric Expansion of a Supersonic Stream," *Acta Astronautica,* Vol. 9, 1982, pp. 333-338.

[5]Goethert, B.H., *Transonic Wind Tunnel Testing,* Pergamon Press, London, 1961, pp. 70, 270.

[6]Schlichting, H., *Boundary Layer Theory,* 6th Ed., McGraw-Hill Book Co., New York, 1968, p. 367.

[7]Carafoli, E., *High Speed Aerodynamics,* Editura Technica, Bucharest, Romania, 1956, pp. 312-314.

[8]Sears, W.R., *General Theory of High Speed Aerodynamics,* Vol. VI, Princeton University Press, Princeton, NJ, 1954, pp. 453-457.

[9]Van Dyke, M.D., "Second-Order Slender Body Theory—Axisymmetric Flow," NASA TR R-47, 1959, pp. 9-10.

Transient Temperature Distributions in a Radiantly Heated Hollow Cylinder

Y. Sakurai*
Mitsubishi Electric Corporation
Kamakura, Japan
and
D.K. Edwards†
University of California, Irvine, California

Introduction

A HOLLOW cylinder is a common structural element in a spacecraft, e.g., in booms, struts, and antennas. Therefore, the thermal behavior of such an element in the space environment is of some interest, especially since the circumferential temperature distribution affects its deflection and state of stress. Parts of the problem have been addressed previously. Olmstead[1] treated the transient response 20 years ago without regard for internal radiation. Steady-state analyses were made by Charnes and Raynor[2] and Nichols[3] with allowance for wall conduction and external radiation, but for no internal heat exchange. Sparrow and Krowech[4] treated internal convection into an opaque fluid. Hrycak and Helgans[5] considered internal radiation correctly for a black interior and neglected radial thermal resistance. Edwards[6] allowed for radial resistance and a nonblack wall.

This Note treats the transient temperature distribution around a spinning hollow thin-walled cylinder with arbitrary initial temperature and allowance for internal and external thermal radiation transfer. Sample calculations show the effect of time from startup and spin rate on the temperature profile.

Formulation

A cylinder of mean radius R and thin-wall thickness b is shown in Fig. 1. For the thin wall, the wall temperature may be assumed to be uniform over thickness. The heat conduction equation with radiative boundary conditions is then written as a fin equation:

$$\rho cb\frac{\partial T}{\partial t}=\frac{kb}{R^2}\frac{\partial^2 T}{\partial\theta^2}-(q_e+q_i)+q_a \tag{1}$$

Here q_e is the externally emitted heat flux, $\epsilon_e\sigma T^4$ in deep space, q_i is the net heat flux into the interior, and q_a the externally absorbed flux. The net internal flux is the difference between the radiosity q^+ and irradiation q^-

$$q_i=q^+-q^- \tag{2}$$

where

$$q^+=\epsilon_i\sigma T^4+(1-\epsilon_i)q^- \tag{3}$$

$$q^-(\theta)=\int_{-\pi}^{+\pi}q^+(\theta')K(\theta,\theta')\mathrm{d}\theta' \tag{4}$$

Received Aug. 31, 1984; revision received March 25, 1985.

*Member of the Technical Staff, Kamakura Works; currently Visiting Scholar, University of California, Irvine, CA. Member AIAA.

†Professor and Chairman, Department of Mechanical Engineering. Member AIAA.